NUMERICAL SIMULATION OF AN URBAN BOUNDARY LAYER OVER FLAT TERRAIN

by VYAS PANDEY, *Department of Geophysics, Banaras Hindu University, Varanasi-221 005*

and

MURARI LAL, *Meteorological Office, Poona-411 005*

(*Received 6 April 1978: after revision 3 Juiy 1978*)

A two-dimensional time-dependent boundary layer model has been developed to study the air flow over urban regions. The model incorporates a soil layer and the surface temperature is determined from the heat budget equation, It assumes hydrostatic equilibrium and uses the continuity equation in its incompressible form. Eddy exchange coefficients of momentum and heat are parameterized. The model in its present form does not incorporate humidity or radiative effects.

The model has been applied to simulate air flow over urban areas with flat terrain. The results indicate that the model is capable of simulating the observed temperature structure (including the elevated cooling associated with elevated inversions and the warming above the layer of elevated cooling) over the cities during night time. The elevated cooling is largely due to the upward vertical velocities near the leading edge of the city induced by the city's obstruction to the prevailing synoptic flow.

INTRODUCTION

THE ATMOSPHERIC layer extending from surface to about 1500 m high is known as the planetary boundary layer. Much of the atmosphere's heat and water vapour are transported through turbulent transfer processes in this layer. The process of urbanization inadvertently modifies various meteorological parameters such as temperature, wind, humidity and cloudiness within the atmospheric boundary layer. In principle, observational studies could provide the degree of understanding of the modifications of local weather by metropolitan cities required for intelligent urban planning. However, the amount of money, manpower and time required for such studies are often prohibitive and hence these studies must be supplemented by theoretical modelling studies. In view of this, a two-dimensional numerical model is developed which simulates the thermal structure of the urban boundary layer.

The model includes a soil layer and the governing equations in primitive forms are solved in the model by employing finite difference techniques. The umerical schemes used in this model enable it to be applied with or without the use of a constant flux layer near the surface. If constant fluxes of momentum and heat are not assumed near the surface, the transition layer equations are applicable right down to the surface. The model assumes hydrostatic equilibrium and uses the equation of continuity in its incompressible form. The justification for the use of hydrostatic assumption is usually provided on the grounds of a dimensional criterion (Haltiner 1971). Further, the incompressibility of the air is justified since the model's extent is less than 2 km in the vertical. Soil and surface parameters can vary along the horizontal.

Eddy exchange coefficients of momentum and heat are parameterized. In the following text, the equations governing the model in the transition, constant flux and soil layers are given.

Model Equations

Since the model is restricted to two space dimensions, homogeneity is assumed along one of the horizontal axes. However, the wind velocity is three-dimensional as the coriolis force is taken into account. In addition to the hydrostatic and incompressibility assumption, the following assumptions are used : in comparison with the turbulent diffusivity molecular viscosity is neglected, and the atmosphere is considered dry and radiative effects are neglected.

The transition layer equations, with the above assumptions, are usually written as

$$\left.\frac{\partial u}{\partial t}\right)_z = -\left.v\frac{\partial u}{\partial y}\right)_z - w\frac{\partial u}{\partial z} + f(v-v_g) + \frac{\partial}{\partial z}\left(K_{mz}\frac{\partial u}{\partial z}\right) + K_{my}\left(\frac{\partial u^2}{\partial y^2}\right)_z \quad (1)$$

$$\left.\frac{\partial v}{\partial t}\right)_z = -\left.v\frac{\partial v}{\partial y}\right)_z - w\frac{\partial v}{\partial z} + fu - c_p\,\theta\left.\frac{\partial P}{\partial y}\right)_z + \frac{\partial}{\partial z}\left(K_{mz}\frac{\partial v}{\partial z}\right) + K_{my}\left(\frac{\partial^2 v}{\partial y^2}\right)_z \quad \ldots(2)$$

$$\left.\frac{\partial \theta}{\partial t}\right)_z = -\left.v\frac{\partial \theta}{\partial y}\right)_z - w\frac{\partial \theta}{\partial z} + \frac{\partial}{\partial z}\left(K_{\theta z}\frac{\partial \theta}{\partial z}\right) + K_{\theta y}\left(\frac{\partial^2 \theta}{\partial y^2}\right)_z \quad \ldots(3)$$

$$\frac{\partial v}{\partial y} + \frac{\partial w}{\partial z} = 0 \quad \ldots(4)$$

$$\frac{\partial p}{\partial z} = -g/c_p\,\theta \quad \ldots(5)$$

$$P = \rho RT \quad \ldots(6)$$

$$T = P.\theta \quad \ldots(7)$$

In the above equations, x and y are the two horizontal axes and z is the vertical coordinate while t is the time. The subscript z is used to denote a derivative along a constant z surface. The eastward (x-) and northward (y-) components of the wind velocity are represented by u and v respectively while the vertical velocity is represented by w. The subscript g is used to denote the geostrophic wind speed. The coriolis parameter is denoted by f. K_{my} and K_{mz} are the eddy exchange coefficients for momentum along the y direction and vertical direction respectively. The variables θ and p are potential temperature and pressure respectively. Further, $P \equiv (p/p_0)^{R/c_p}$, where R is the gas constant and c_p is the specific heat of air at constant pressure. $K_{\theta z}$ and $K_{\theta y}$ are the coefficients of eddy diffusivity for heat along the verti-

cal and y directions respectively. T is the temperature, g is the acceleration due to gravity and ρ is the density.

The parameterized expressions for the eddy exchange coefficients used in this study are as given below :

$$\left.\begin{aligned} &\Gamma (z + z_0)^2 \left(\frac{g}{\theta}\right)^{1/2} \left|\frac{\partial \theta}{\partial z}\right|^{1/2}, && \text{for } R_i \leqslant -0.048 \\ &l^2 S_w (1 + \alpha R_i)^2, && \text{for } R_i > -0.048 \\ &K_{mz} = K_{\theta z} = K(z) \\ &\qquad l^2 S_w (1 - R_i)^{-2}, \text{ for } R_i > 0. \end{aligned}\right\} \quad \ldots(8)$$

where

$$S_w \equiv \left\{\left(\frac{\partial u}{\partial z}\right)^2 + \left(\frac{\partial v}{\partial z}\right)^2\right\}^{1/2},$$

l is the mixing length, R_i is the Richardson number, z_0 is the roughness length, Γ and α are constants (0.9 and -3 respectively). The mixing length, l is specified by using the empirical expression, as given by Blackadar (1962).

$$l = \frac{k_0 (z + z_0)}{1 + k_0 (z + z_0)/\lambda}$$

where $\lambda = 0.0004\ U_g f^{-1}$. Here U_g is the geostrophic wind speed and k_0 is Von Karman constant. The above expressions are assumed to be valid up to about 60 to 80 m height depending upon the model's extent and vertical resolution.

Above about 60 to 80 m height a profile formulation for K is used, using an interpolation formula suggested by O'Brien (1970). This formula is given as ;

$$K(z) = K(z') + \frac{(z - z')}{(z' - h')}\left\{K(h') - K(z') + (z - h')\left[\left(\frac{\partial K}{\partial z}\right)_{h'} + \frac{2(K(h) - K(z'))}{(z' - h')}\right]\right\}, \quad \ldots(9)$$

where z' is the height at which the value of $K(z)$ has decreased to a small value and h' is the height up to which eqn. (8) is valid.

The horizontal eddy exchange coefficients for momentum and potential temperature (K_{my} and $K_{\theta y}$) are assumed to be equal and constant. The value of the constant (K_y) used in our study ranges from 250 to 1000 $m^2 s^{-1}$ depending on the grid interval.

In using the finite difference schemes to solve the transition layer equations nonuniform vertical grid spacing is employed since the vertical profiles of wind and temperature exhibit strong gradients near the surface of the earth but relatively weak gradients at the higher levels. However, because of the presence of the second derivatives in the turbulent diffusion terms, the use of non-uniform grid spacing may lead to

inaccurate results. This can be avoided by making a coordinate transformation in the vertical to a new independent variable for which uniform grid spacing can then be used. In the present study the following transformation is used :

$$\zeta = \ln \frac{(H\phi + 0.01)}{0.01} + \frac{H\phi}{30}.$$

The model extends up to H above local surface (i.e., $H + h$ from reference surface). This log-linear transformation is chosen arbitrarily but it gives good resolution throughout the model's vertical extent.

In addition to the coordinate transformation a constant flux layer near the surface is also used which extends up to about 40 m above the local surface. In this layer the following profile equations are used ;

$$v = U_*\left\{\frac{1}{k_0} \ln \frac{(z + z_0)}{z_0} + \frac{z}{\lambda} - \alpha \frac{g}{\theta_0} \frac{\theta_*}{U_*^2} z\right\}$$

and

$$\theta - \theta_0 = \theta_* \left\{\frac{1}{k_0} \ln \frac{(z + z_0)}{z_0} + \frac{z}{\lambda} - \alpha \frac{g}{\theta_0} \frac{\theta_*}{U_*^2}\right\} \text{ for } R_i \geqslant -0.048.$$

For $R_i < -0.048$,

$$v = -3\,\Gamma^{-2/3} U_*^{5/3} \left(\frac{g}{\theta_0}\right)^{-1/3} . \theta_*^{-1/3} [(z + z_0)^{-1/3} - z_0^{-1/3}]$$

and

$$(\theta - \theta_0) = -3\,\Gamma^{-2/3}\, U_*^{2/3} . \theta_*^{2/3} . \left(\frac{g}{\theta_0}\right)^{-1/3} [(z + z_0)^{-1/3} - z_0^{-1/3}]$$

In the above equations U_* and θ_* are frictional velocity and frictional potential temperature respectively, while V is the wind speed and θ_0 is the potential temperature at the surface.

The temperature at the soil-air interface is obtained by energy-budget equation. To take into account the effect of variation of the soil temperature on the heat budget at the air-earth interface a time-dependent equation of heat diffusion in the soil layer is used which is as follows :

$$\frac{\partial T_s}{\partial t} = K_s \frac{\partial^2 T_s}{\partial z_s^2}, \qquad \ldots(10)$$

where K_s is the soil thermal diffusivity, T_s is the soil temperature and z_s is the vertical coordinate in the soil layer with $z_s = 0$ at the soil-air interface and $z_s = -D$ at the lower boundary of the subsurface layer. Using a coordinate transformation $\eta = \ln (c - z_s)$, where c is chosen equal to 0.015 m, eqn. (10) may be written as

$$\frac{\partial T_s}{\partial t} = \frac{K_s}{(c - z_s)^2}\left[\frac{\partial^2 T_s}{\partial \eta^2} - \frac{\partial T_s}{\partial \eta}\right] \qquad \ldots(10a)$$

Numerical Procedure

The surface layer equations in the model are solved analytically while the equations in the transition layer are solved by the use of an explicit finite difference scheme (Richtmyer & Morton 1967). The finite difference scheme used to approximate the advection terms to solve the equations in the transition layer is the 'Upstream or Upwind Differencing Scheme'. Forward differences are adopted in time. The stability criterion for this scheme is that the Courant number, $c \equiv v. \triangle t/\triangle y$, should be less than or equal to unity. This scheme possesses a transportive property and is conservative as long as velocity components do not change sign. The slope $\partial h/\partial y$ is computed using the second order finite difference approximtion, i.e., as $(h_{i+1} - h_{i-1})/2\ \triangle y$. The diffusion terms are approximated by the centered differences. A time step restriction applies to the diffusion terms since the scheme is explicit. The stability condition is : $2K_d \triangle t/\triangle s^2 < 1$, where $\triangle s$ is the space grid interval in any direction and K_d is the eddy diffusion coefficient in the corresponding direction. The overall time step of the scheme is determined by the combined effects of advection and diffusion terms. A time step of 60 seconds was used in our simulation. The finite difference scheme used for the subsurface temperature equation is that which was termed 'hopscotch' scheme by Gourlay (1970).

The top of the model is set at 1000 m in performing the sensitivity analysis. Fifteen levels are used with a grid interval $(\triangle)\zeta$ of 3,20.3305 in the vertical. The corresponding values of height z are given in Table I. Six levels (including the air-soil interface) are used in the soil layer. The corresponding values of depths are given in Table II. The horizontal grid interva used was 2 km with 30 grid points.

Table I

Heights above local surface corresponding to the vertical grid levels used in the atmospheric layer

Grid number	Height in metres
1	0.00
2	0.23
3	5.11
4	39.69
5	106.26
6	185.63
7	270.40
8	358.12
9	447.53
10	538.10
11	629.50
12	721.49
13	813.98
14	906.84
15	1000.00

TABLE II

Depths corresponding to the grid levels used in the soil layer.
(Depths are from air-soil interface)

Grid number	Depth in metres
1	0.000
2	0.015
3	0.045
4	0.105
5	0.225
6	0.465

The model described above has been used to investigate the wind and thermal structure of the urban boundary layer over flat terrain and the results are presented in the following paragraphs.

SIMULATION RESULTS

This experiment has been conducted using the initial conditions corresponding to a northerly geostrophic wind of speed 5 m s^{-1} (Fig. 1) and the horizontal distribution of the urban (surface and soil) parameters shown in Table III. The results of the above experiments are shown in Figures 2 through 6 at 5 hours and 9 hours after sunset. Figs. 2*a–b* show the distribution of potential temperature. A distinct heat island, whose strength decreases with height, can be seen in the urban area (region A). The vertical temperature distribution at the upwind rural boundary is characterized by strong inversion near the surface whose strength increases with time after sunset. As regards the temperature structure over the urban area slightly superadiabatic lapse rates can be seen in the central area of the city (the shaded area in

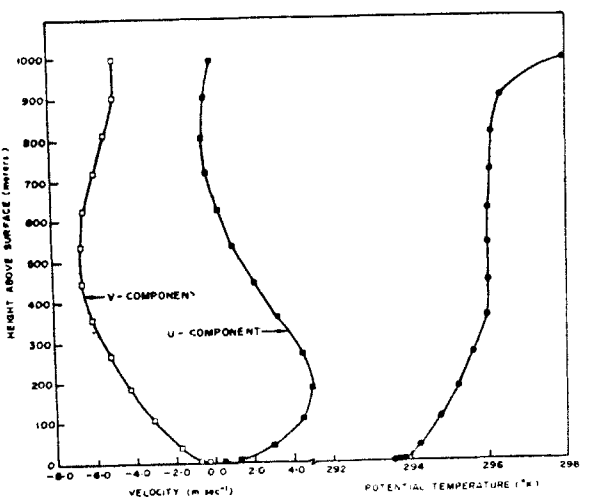

FIG. 1. Initial profiles of wind and potential temperature.

TABLE III

Assumed variation of roughness length, artificial heat flux and soil thermal diffusivity along the horizontal in the present study. To get the thermal conductivity of the soil the values of thermal diffusivity are to be multiplied by thermal capacity ($\rho_s c_s = 2093000$).

Grid unit starting from the upwind lateral boundary	Roughness length (z_0) in metres	Artificial heat flux in $W\ m^{-2}$	Thermal diffusivity of soil (K_s) in $m^2 s^{-1} \times 10^6$
1 to 2	0.05	0.0	0.5
3	1.00	30.0	0.8
4	1.50	60.0	1.0
5	2.00	84.0	1.5
6	2.50	108.0	1.8
7	3.00	120.0	2.0
8	3.00	120.0	2.0
9	3.00	120.0	2.0
10	2.50	108.0	1.8
11	2.00	84.0	1.5
12	1.50	60.0	1.0
13	1.00	30.0	0.8
14 to 30	0.05	0.0	0.5

region A of Figs. 2*a–b*) from the surface to about 50 m height. Above the region A, a strong stability similar to that of the upwind rural boundary can be noticed. It can also be noted that the temperature over the city in the region of elevated inversion is cooler than at the corresponding height over the upstream rural boundary. This elevated cooling and the plume structure of the heat island can be more clearly seen in Figs. 3*a–b* (region B) where the deviations of potential temperature from the values at the upstream rural boundary are shown. Above this elevated cooling (region C in Figs. 3*a–b*) the temperature over the city is once again warmer than that at the same height over the upwind lateral boundary.

The vertical distribution of the horizontal wind speed at the upwind lateral boundary is shown in Fig. 4. This distribution together with the distribution of the perturbations of the horizontal wind speed (Figs. 5*a–b*) describe the distribution of the horizontal wind speed over the city. The distribution of the perturbation of wind speed shows a decrease at lower levels over the city, while at higher levels it shows an increase. The decrease in wind speed extends to higher levels on the windward side of the city than on the leeward side of the city.

The distribution of vertical velocity (Figs. 6*a–b*) shows upward motion near the leading edge of the city. Downward motion can be noticed over the rest of the city at 5 hours after the sunset. At 9 hours after sunset, the upward motion near the leading edge of the city extends towards the centre of the city. At higher levels the downward motion extends towards the center of the city, while over the trailing edge of the city the downward motion is replaced by upward motion. Further, it can be seen that the vertical velocities at this time are generally weaker than those at 5 hours after sunset.

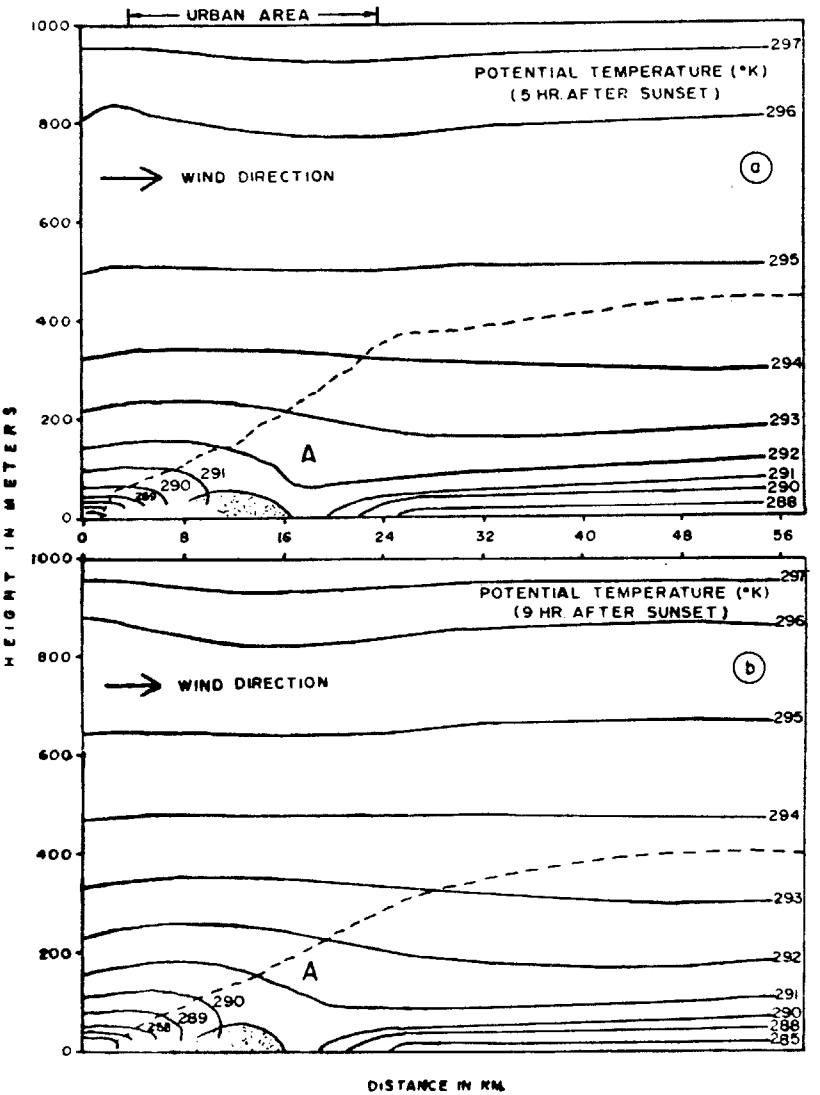

FIG. 2*a-b*. Potential temperature distribution at 5 and 9 hours after sunset (flat terrain). The dashed curve marking the boundary of region A represents zero potential temperature perturbation.

These results simulate very well the complex picture of observed temperature and horizontal wind fields over urban cities. The cause for the decrease in the horizontal wind speed near the surface in the urban region is obviously the increased friction. The increase in wind speed aloft is the direct result of the need to satisfy continuity. The causes of the formation of the heat island are artificial heat, increased mixing over the city (giving downward heat transport due to temperature inversion) and the increased thermal diffusivity and conductivity of the surface in the urban area. In the real atmosphere additional causes such as increased downward longwave radia-

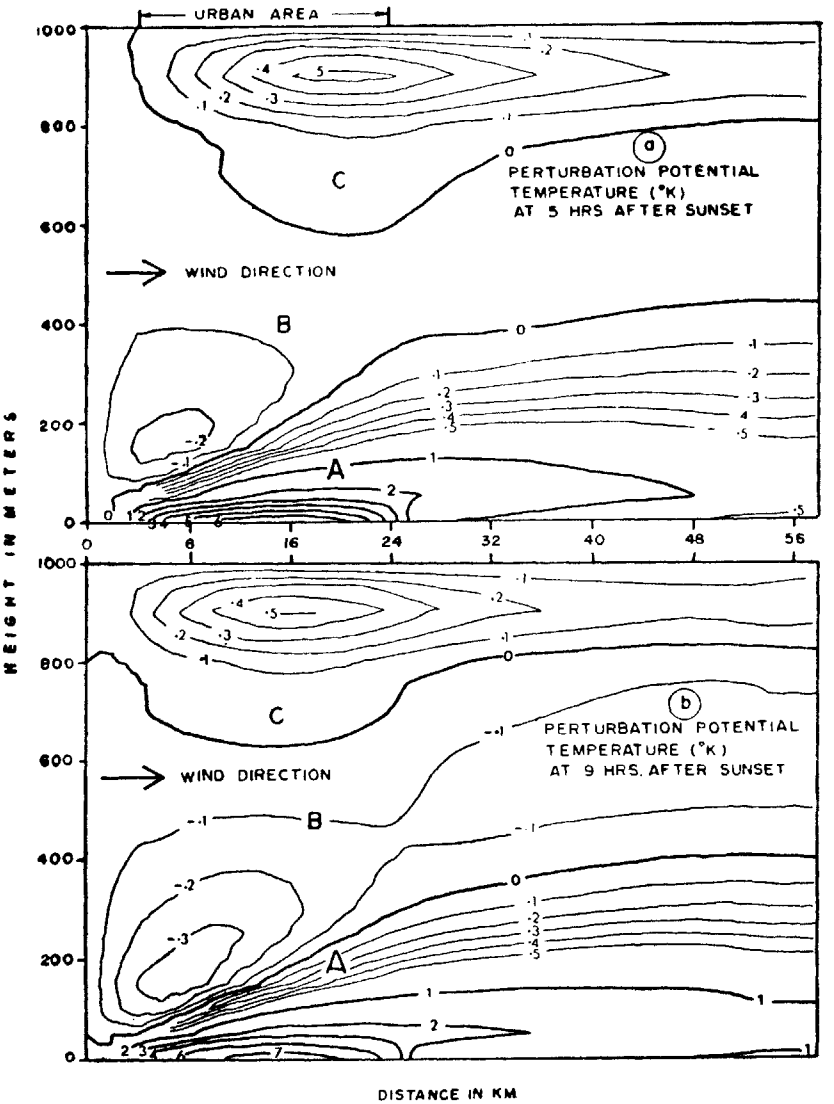

FIG. 3*a-b*. Distributions of perturbation potential temperature at 5 and 9 hours after sunset (flat terrain).

tion from pollutants in the atmosphere and release of latent heat of condensation may also influence the strength of the heat island.

As air from the upwind rural area (whose temperature profile is characterized by inversion) moves over the city it is modified strongly at the lower levels (see region A in Figs. 2*a–b*) to give rise to unstable or less stable lapse rates. Above the level of this modification the air retains its rural characteristic of inversion or strong stability. However, the temperature profile in this region of elevated inversion (being cooler) does not exactly coincide with that of the upwind rural region at the same height. Upwind vertical velocities at the leading edge of the city could be the major cause of

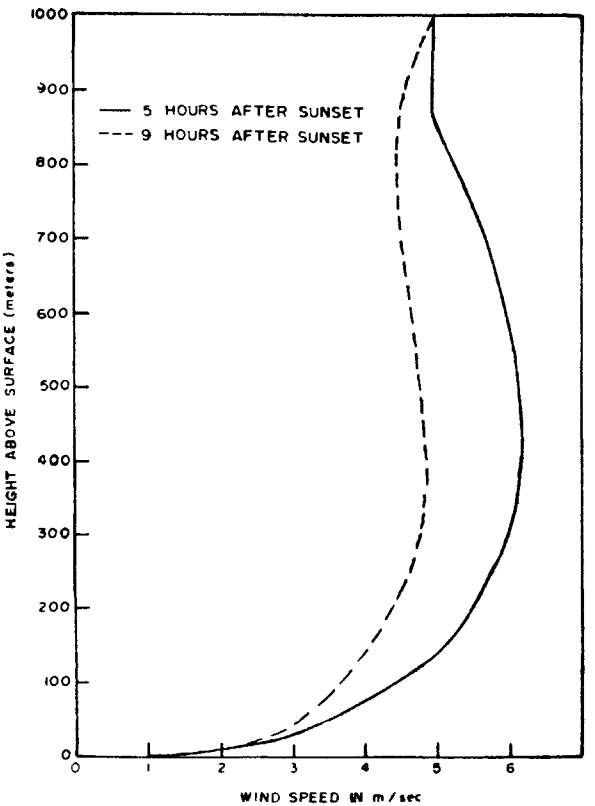

FIG. 4. Wind speed distribution at the lateral boundary (flat terrain).

this elevated cooling. These upward vertical velocities are the result of the city's partial obstruction to the approaching flow. Although small in magnitude, the upward vertical velocities advect cooler air upwards under inversion conditions. This results in elevated cooling over the city (region B in Figs. 3*a–b*) after subsequent downstream advection of the modified ar. In an attempt to return to normal flow downward motion occurs downwind of the upward motion at the leading edge of the city. This downward motion can bring warm air to give rise to a slightly warmer region (see region C in Figs. 3*a–b*) above the elevated cooling.

The general weakening of the vertical velocities with time is due to the decrease in the background flow shown in Fig. 4. Although vertical velocities are generally weaker at 9 hours after sunset the elevated cooling is relatively stronger than that at 5 hours after sunset. The reason is partly the weakening of the downdraught over the city and partly the intensification of the upwind rural inversion.

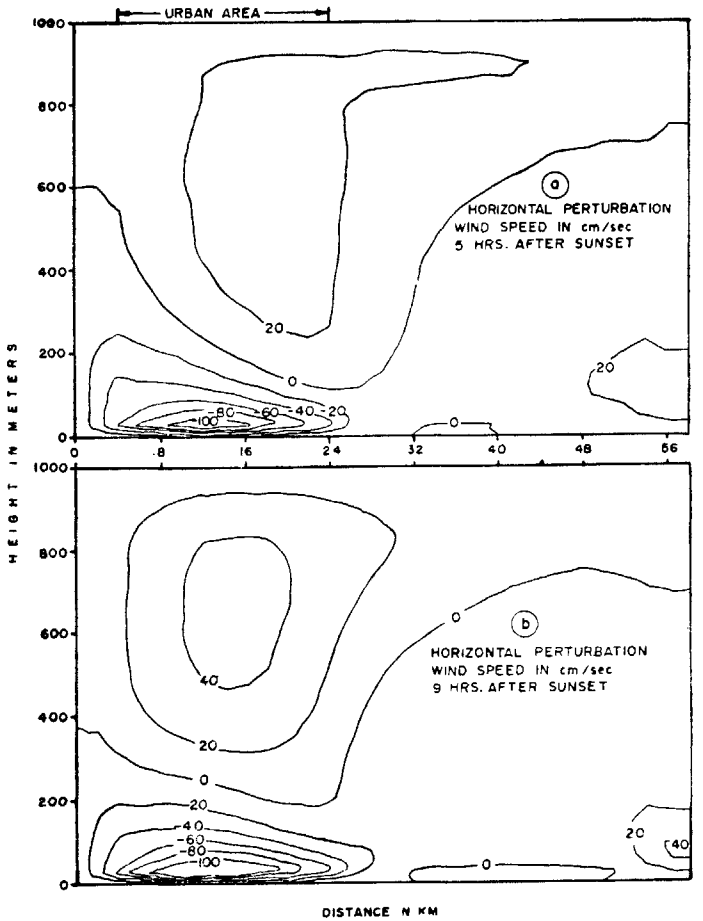

FIG. 5*a-b*. Distributions of horizontal perturbation wind speed at 5 and 9 hours after sunset (flat terrain).

CONCLUSIONS

The foregoing discussions indicate that the model has been successful in predicting the full observed temperature structure over the cities during night time. The predicted wind field is also consistent with observations. A sensitivity analysis of the model reveals that inversion to slightly superadiabatic conditions can exist near the surface in the city when the outlying upwind rural areas exhibit strong inversions. Even if unstable lapse rates prevail at lower levels in the urban areas the temperature structure at higher levels shows inversion or stability similar to that of upwind rural area. The region of this elevated inversion over the city is slightly colder than that of the rural area. Above the layer of elevated cooling the air over the urban area is once again warmer than that over the upwind rural area.

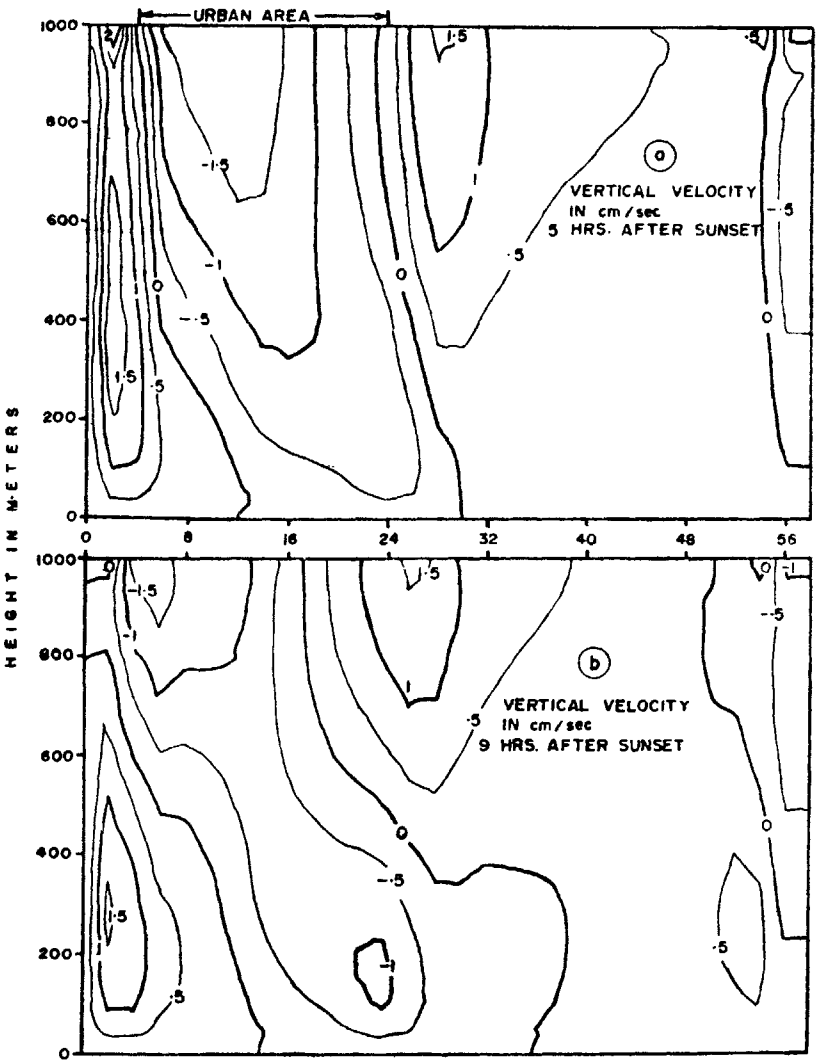

FIG. 6*a-b*. Vertical velocity fields at 5 and 9 hours after sunset (flat terrain)

ACKNOWLEDGEMENTS

The Council of Scientific and Industrial Research, New Delhi provided financial support to one of the authors (V.P.) in the form of a junior research fellowship.

REFERENCES

Blackadar, A. K. (1962). The vertical distribution of wind and turbulent exchange in a neutral atmosphere. *J. geophys. Res.*, **67**, 3095–3102.

Gourlay, A. R. (1970). Hopscotch : A fast second order partial differential equation solver. *J. Inst. Maths. Applics.*, **6**, 375–390.

Haltiner, G. J. (1971). *Numerical Weather Prediction.* Wiley N.Y., 317 pp.

O'Brien, J. (1970). On the vertical structure of the eddy exchange coefficient in the planetary boundary layer. *J. atmos. Sci.*, **27**, 1213–1215.

Richtmyer, R. D., and Morton, K. W. (1967). *Difference Methods for Initial Value Problems.* Wiley-Interscience, N.Y., 405 pp.